Scientific Visualization, 2023, volume 15, number 3, pages 101 - 107, DOI: 10.26583/sv.15.3.11

Mueller-Matrix Stress Mapping in TeO_2 Crystals Under Dynamic Loading

D.D. Khokhlov[1,A,B], A.A. Bykov[2,A,B], A.Yu. Marchenkov[3,A], Yu.V. Pisarevsky[4,C], Ya.A. Eliovich[5,C], V.I. Akkuratov[6,C], A.A. Khvostov[7,A]

[A] National Research University "Moscow Power Engineering Institute"
[B] Scientific and Technological Center of Unique Instrumentation RAS
[C] FRC «Crystallography and Photonics» RAS

[1] ORCID: 0000-0003-0919-7762, khokhlov.dd@ntcup.ru
[2] ORCID: 0000-0002-7574-3437, bykov@ntcup.ru
[3] ORCID: 0000-0002-0806-7336, art-marchenkov@yandex.ru
[4] ORCID: 0000-0003-0013-0019, yupisarev@yandex.ru
[5] ORCID: 0000-0002-1836-0579, yan.eliovich@gmail.com
[6] ORCID: 0000-0002-2780-6456, akkuratov.val@gmail.com
[7] ORCID: 0009-0005-5774-5905, KhvostovAA@mpei.ru

Abstract

Components of optoelectronic devices installed in aircrafts and space vehicles experience significant mechanical loads during their operation. Excessive and cyclic loads may lead to the defect growth or the fatigue failure. In this paper, we describe a non-destructive imaging technique for stress mapping in anisotropic crystalline materials during bench test. The technique is based on Mueller-matrix imaging and the material photoelasticity. The results of experimental studies for two observation directions coinciding with different crystallographic axes of TeO_2 are presented. Main limitations and further potential development of the technique are discussed.

Keywords: crystalline materials, crystal TeO_2, non-destructive testing, Mueller-matrix imaging, computational imaging, mechanical stress visualization.

1. Introduction

Optical components made of crystalline materials are widely in use in optical instrumentation [1, 2]. The key parts of acousto-optical devices include anisotropic crystalline materials. Quality and performance of these components affect the accuracy, reliability and operation cycle duration of the entire complex instruments. This paper addresses the development of nondestructive testing methods for detection of the mechanically stressed zones appearing in crystalline materials under external mechanical loads. Formation of the zones of mechanical stress localization may lead to the defect growth or the fatigue failures. Stress concentration zones are caused by the crystal growth technology violations and excessive or cyclic mechanical loads typical for onboard optoelectronic devices installed in aircrafts and space vehicles. The former case involves the post-production quality control via state-of-art crystallographic techniques [3, 4] but the latter implies simulations and bench tests to assess the crystalline component performance [5, 6]. We propose to apply Mueller-matrix polarization-sensitive imaging [7] technique for nondestructive visualization of stress concentration zones during the bench tests of crystalline optical components.

2. Experimental setup

Experimental setup for crystalline optical components mechanical bench tests includes universal testing machine (Instron 5982) and Mueller-matrix imaging system. The testing

machine provides the controlled uniaxial compression of a crystalline specimen installed between press plates with a specialized floating hinge. To demonstrate feasibility of the proposed technique we chose an anisotropic material widely utilized in spectral imaging devices and laser instrumentation [8-12], tetragonal form of tellurium dioxide α-TeO_2. Layout of the experimental setup is shown in figure 1.

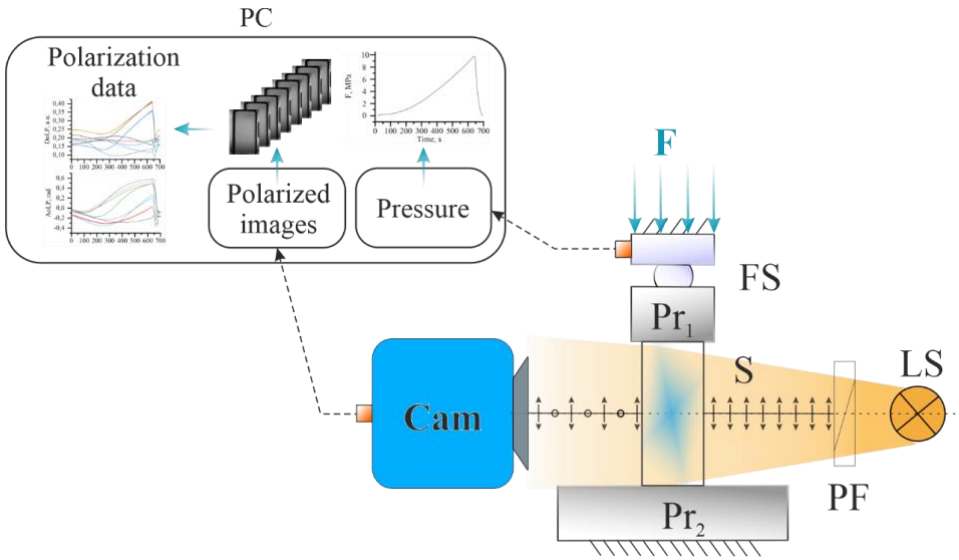

Figure 1. Experimental setup. Cam - camera, Pr_1 and Pr_2 - press plates, FS - floating hinge, PF - polarizing filter, LS - light source, F - compression force applied to press plate, S – sample

The Mueller-matrix imaging system consists of LED-based broadband light source, polarizing filter and polarization-sensitive camera (The Imaging Source DZK 33UX250). Specimen installed in the universal testing machine is illuminated by the linearly polarized light. The camera image sensor is equipped with a specific polarization filter array. Four types of filters with the plane of polarization turned at an angle of 0°, 45°, 90° и 135° to the direction of image sensor pixel rows are arranged at 2×2 pixel blocks. According to Malus's law, during image acquisition each pixel block exposed by the linearly polarized light with arbitrary orientation of polarization direction will provide four different intensity values (I_0, I_{45}, I_{90}, I_{135}). Thus, the camera allows simultaneous image acquisition in four polarization directions. Using the acquired intensity values one can evaluate the parameters of Stokes vector $\vec{S} = \left(S_0, S_1, S_2, S_3\right)^T$ for each 2×2 pixel block as follows:

$$S_0 = I_0 + I_{90},$$
$$S_1 = I_0 - I_{90},$$
$$S_2 = I_{45} - I_{135}.$$

Taking into account the linear polarization of the illumination, the parameter S_3 describing circular polarization can be excluded from consideration. For quantitative analysis of the light passing through the specimen we calculated the spatial distributions of two values: Degree of Linear Polarization (DoLP) showing the ability of the specimen material to conserve the linear polarization of light and Angle of Linear Polarization (AoLP) associated with the polarization direction. DoLP and AoLP may be defined using the Stokes vector parameters:

$$\mathrm{DoLP} = \frac{\sqrt{S_1^2 + S_2^2}}{S_0},$$

$$\mathrm{AoLP} = \arctan\frac{S_2}{S_1}.$$

Without the specimen the polarization-sensitive camera illuminated with collimated linearly polarized light delivers spatially homogeneous DoLP and AoLP maps. During the external mechanical load increases, local deviations of the mentioned values appearing and developing in the investigated anisotropic specimen zone indicate the stress localization as the excessive stress leads to the additional retardation introduced according to the stress-optic law [13, 14]. Stress localization zones are associated with the structural inhomogeneities (defects) in crystalline material [15]. Therefore, analysis of DoLP and AoLP spatial distributions may provide the defect detection during bench tests.

3. Results

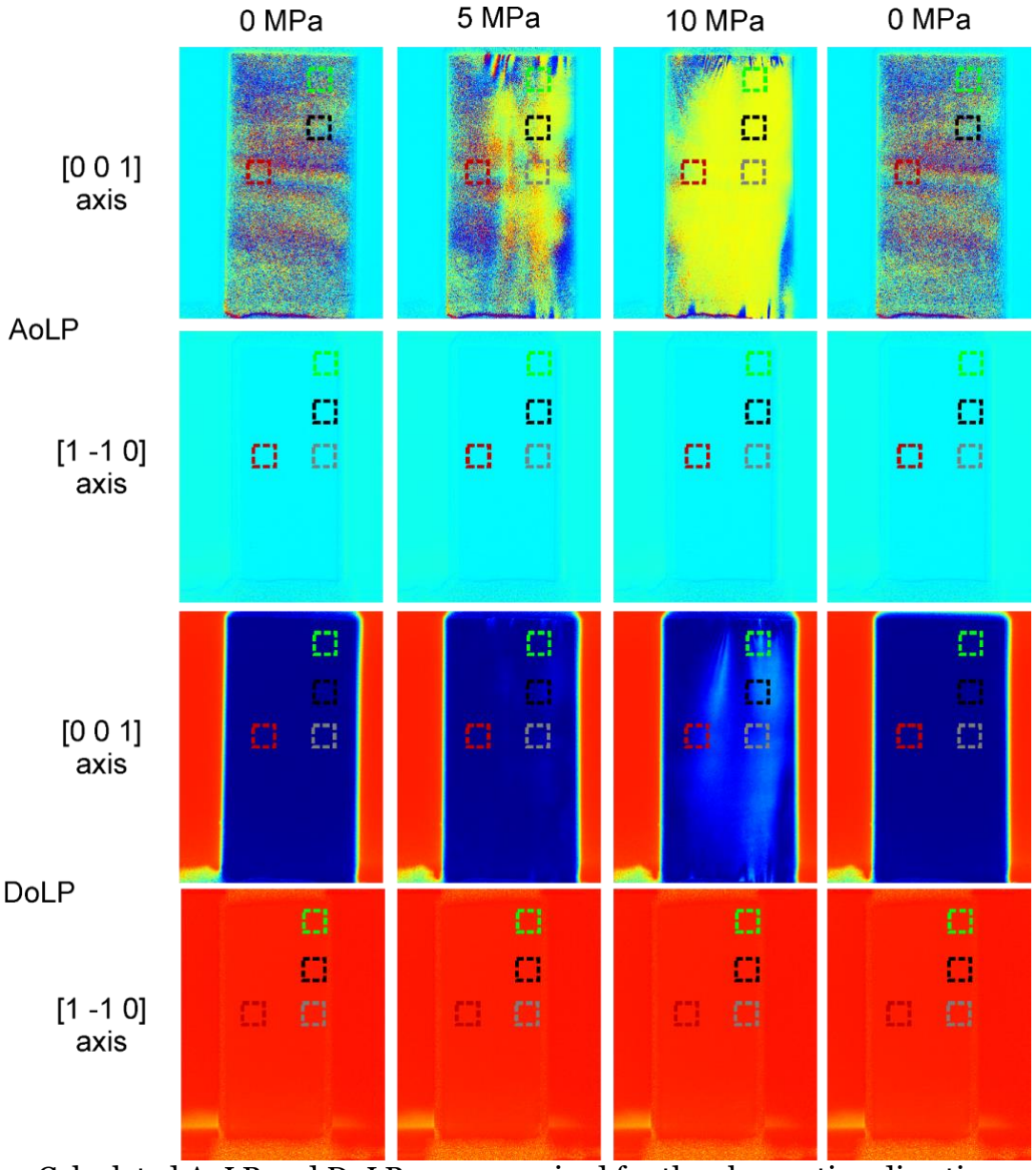

Figure 2. Calculated AoLP and DoLP maps acquired for the observation direction coincident to the crystallographic axis [0 0 1] (two upper rows) and [1 -1 0] (two lower rows)

Experimental testing involved TeO_2 specimen with dimensions of 20,1×8,9×9,6 mm. The compression force direction coincided with the direction of the crystallographic axis [1 1 0]. The external mechanical load monotonically increased from 0 to 10 MPa and afterwards decreased 0 MPa. The observation direction was aligned coincident to [0 0 1] and [1 -1 0]

crystallographic axes in two independent tests. During the entire experimental tests, the Mueller-matrix imaging system continuously performed image acquisition at 40 fps frame rate.

At the image processing stage, we calculated the timed stacks of DoLP and AoLP maps. Examples of the calculated maps are shown in figure 2. To demonstrate quantitative time dependencies of DoLP and AoLP in particular spatial zones the images were splitted into separate regions of 40×40 pixels. Time dependencies of DoLP and AoLP mean values for the most remarkable regions are demonstrated in figure 3.

4. Discussion

Spatial maps acquired for [0 0 1] axis demonstrate significant difference between the unloaded specimen and the background. Low values of DoLP and speckle pattern at AoLP map are associated with gyrotropy, which manifests in rotation of the polarization plane of light propagating along the optical axis [0 0 1] of TeO_2 [17]. The angle of rotation considerably depends on the light wavelength. Therefore, the linearly polarized broadband light transforms into the unpolarized after passing the specimen. Increasing external mechanical load and resulting uneven stress distribution lead to the rise of the stress-induced birefringence which causes the appearance of spatial zones with higher DoLP and explicit AoLP values. Spatial maps for [1 -1 0] axis demonstrate no notable changes.

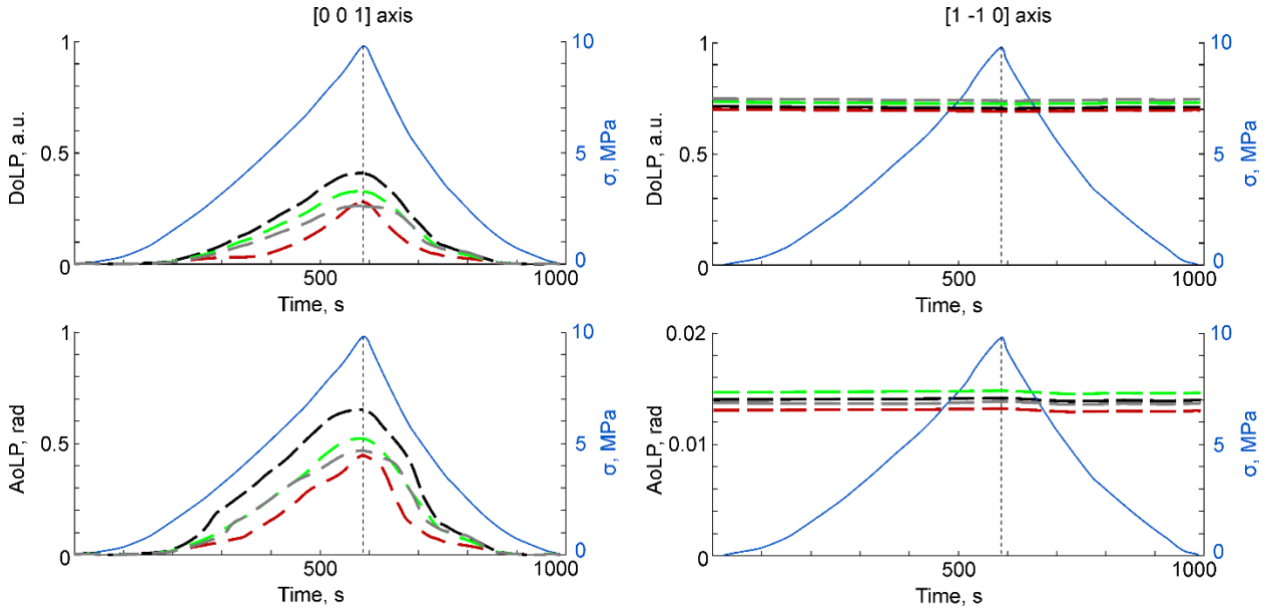

Figure 3. Temporal DoLP (top) and AoLP (bottom) dependencies. Colours of the curves correspond to the frame colours in Figure 2.

The similarity of DoLP and AoLP maps and equal levels of DoLP and AoLP values in the beginning and in the end of the experiment highlight the absence of irreversible structural failures in the specimen. For [0 0 1] axis, extrema locations of DoLP and AoLP curves correspond to the maximum of the external mechanical load. Stress concentration zones demonstrate earlier and more intensive gain of the measured values. Curves obtained for [1 -1 0] axis confirm the ability of the specimen material to conserve the polarization state of the light propagating in this direction, as it may be also noticed from the corresponding spatial maps. Thus, observation in this direction do not provide enough sensitivity for stress localization mapping.

Broadband illumination increases the contrast of DoLP spatial distributions for image series obtained during observation along TeO_2 optical axis and simultaneously hinder accurate tracking the changes in AoLP values. Using the narrow-band illumination instead of broadband may lower the visible DoLP contrast but allow measurement of polarization plane

rotation angle and evaluation of stress values in accordance with the stress-optic law. Current experimental setup configuration ensure sufficient time resolution, thus the inevitable decrease of radiant flux associated with narrowing the illumination spectral range is to be compensated by gaining the exposure time.

5. Conclusion

The proposed technique and experimental setup provide high-contrast and real-time stress mapping in TeO2 crystal in the case of its observation along the optic axis. High specificity to the observation direction with respect to the crystallographic axes orientation reduces the scope of the technique but simplifies the optical alignment. The described Mueller-matrix imaging setup may be combined with various testing machines to implement the desired test scenario. Experimental setup with broadband illumination provides considerable DoLP maps contrast that may be an informative stress indicator. More accurate quantitative research requires improving the AoLP mapping. Thus, the perspective research may be devoted to narrow-band Mueller-matrix imaging.

Acknowledgements

This work was performed within the State Assignment of FSRC "Crystallography and Photonics" RAS in the part of samples preparation and was supported by Ministry of Science and Higher Education (grant № 075-15-2021-1362) in the experimental and data processing part.

References

[1] Dmitriev V., Gurzadyan G., Nikogosyan D. Handbook of nonlinear optical crystals / Springer, Berlin, 1999.

[2] Bain A.K. Crystal optics: properties and applications / Wiley, 2019.

[3] Hammond C. The Basics of Crystallography and Diffraction. / Oxford University Press, 2015.

[4] Akkuratov V. I., Blagov A. E., Pisarevskii Y. V., Targonsky A. V., Eliovich Y. A., Moiseeva N. A., Kovalchuk M. V. Time-Resolving X-Ray Acoustic Diffractometry of Perspective Crystalline Materials under Uniaxial Mechanical Loads / Journal of Communications Technology and Electronics, 2021, Vol. 66, Iss. 10, pp. 1184-1188.

[5] Eliovich Y. A., Blagov A. E., Ovchinnikova E. N., Kozlovskaya K. A., Targonskii A. V., Pisarevsky Y. V., Shishkov V. A., Mololkin A. A., Kovalchuk M. V. Accurate Control of Synchrotron Radiation Parameters Using X-ray Acoustic Longitudinal Resonators: Paratellurite (TeO2) Crystals / Crystallography Reports, 2022, Vol. 67, Iss. 7, pp. 1061-1067.

[6] Tretiakov S., Kolesnikov A., Kaplunov I., Grechishkin R., Shmeleva E., Yushkov K. Thermal imaging and conoscopic studies of working acousto-optical devices on the base of paratellurite / International Journal of Thermophysics, 2016, Vol. 37, Iss. 1, pp. 1-9.

[7] Gottlieb D., Arteaga O. Mueller matrix imaging with a polarization camera: application to microscopy / Optics Express, 2021, Vol. 29, Iss. 21, pp. 34723-34734.

[8] Batshev V., Machikhin A., Gorevoy A., Martynov G., Khokhlov D., Boritko S., Pozhar V., Lomonov V. Spectral Imaging Experiments with Various Optical Schemes Based on the Same AOTF // Materials, 2021, Vol. 14, Iss. 11, p. 2984.

[9] Warner A.W., White D.L., Bonner W.A. Acousto-optic light deflectors using optical activity in paratellurite / Journal of Applied Physics, 1972, Vol. 43, Iss. 11, pp. 4489-4495.

[10] Molchanov V.Y., Voloshinov V.B., Makarov O.Y. Quasi-collinear tunable acousto-optic paratellurite crystal filters for wavelength division multiplexing and optical channel selection / Quantum Electronics, 2009, Vol. 39, Iss. 4, p. 353.

[11] Chanover N. J., Voelz D. G., Glenar D. A., Young E. F. AOTF-Based Spectral Imaging for Balloon-Borne Platforms / Journal of Astronomical Instrumentation, 2014, Vol. 3, Iss. 2, p. 1440005.

[12] Korablev O. I., Belyaev D. A., Dobrolenskiy Y. S., Trokhimovskiy A. Y., Kalinnikov Y. K. Acousto-optic tunable filter spectrometers in space missions [Invited] / Applied Optics, 2018, Vol. 57, Iss. 10, pp. C103-C119.

[13] Sampson R. C. A stress-optic law for photoelastic analysis of orthotropic composites / Experimental Mechanics, 1970, Vol. 10, Iss. 5, pp. 210-215.

[14] Dally J. W., Riley W. F., Kobayashi A. S. Experimental stress analysis, McGraw Hill, New York, 1978.

[15] Kolesnikov A.I., Kaplunov I.A., Terent'ev I.A. Defects of different sizes in large paratellurite single crystals / Crystallography Reports, 2004, Vol. 49, pp. 180–183.

[16] Uchida N. Optical properties of single-crystal paratellurite / Physical Review B., 1971, Vol. 4, Iss. 10, p. 3736.

[17] Vorontsova E. Y., Grechishkin R. M., Kaplunov I. A., Kolesnikov A. I., Molchanov V. Y., Talyzin I. V., Tret'Yakov S. A. Manifestation of gyrotropy upon light scattering in paratellurite / Optics and Spectroscopy, 2008, Vol. 104, Iss. 6, pp. 886-889.